

Physical origin of the high energy optical response of three dimensional photonic crystals

Luis A. Dorado¹, Ricardo A. Depine^{1*}, Gabriel Lozano², and Hernán Míguez²

¹*Grupo de Electromagnetismo Aplicado, Departamento de Física, Facultad de Ciencias Exactas y Naturales, Universidad de Buenos Aires, Ciudad Universitaria, Pabellón 1, 1428 Buenos Aires, Argentina*

²*Instituto de Ciencia de Materiales de Sevilla, Consejo Superior de Investigaciones Científicas, Sevilla, Spain*

*Corresponding author: rdep@df.uba.ar

Abstract: The physical origin of the optical response observed in three-dimensional photonic crystals when the photon wavelength is equal or lower than the lattice parameter still remains unsatisfactorily explained and is the subject of an intense and interesting debate. Herein we demonstrate for the first time that all optical spectra features in this high energy region of photonic crystals arise from electromagnetic resonances within the ordered array, modified by the interplay between these resonances with the opening of diffraction channels, the presence of imperfections and finite size effects. All these four phenomena are taken into account in our theoretical approach to the problem, which allows us to provide a full description of the observed optical response based on fundamental phenomena as well as to attain fair fittings of experimental results.

©2007 Optical Society of America

OCIS codes: (050.5298) Photonic crystals; (050.5745) Resonance domain; (160.5293) Photonic bandgap materials

References and links

1. H. Miyazaki and K. Ohtaka, "Near-field images of a monolayer of periodically arrayed dielectric spheres," *Phys. Rev. B* **58**, 6920-6937 (1998).
2. Y. Kurokawa, H. Miyazaki, and Y. Jimba, "Light scattering from a monolayer of periodically arrayed dielectric spheres on dielectric substrates," *Phys. Rev. B* **65**, 201102 (2002).
3. Y. Kurokawa, Y. Jimba, and H. Miyazaki, "Internal electric-field intensity distribution of a monolayer of periodically arrayed dielectric spheres," *Phys. Rev. B* **70**, 155107 (2004).
4. H. Míguez, V. Kitaev, G. Ozin, "Band spectroscopy of colloidal photonic crystal films," *Appl. Phys. Lett.* **84**, 1239-1241 (2004).
5. J. F. Galisteo-López, C. López, "High-energy optical response of artificial opals," *Phys. Rev. B* **70**, 035108 (2004).
6. S. Wong, V. Kitaev, G.A. Ozin, "Colloidal Crystal Films: Advances in Universality and Perfection," *J. Am. Chem. Soc.* **125**, 15589-15598 (2003).
7. K. Wostyn, Y. Zhao, B. Yee, K. Clays, A. Persoons, G. de Schaezen, L. Hellemans, "Optical properties and orientation of arrays of polystyrene spheres deposited using convective self-assembly," *J. Chem. Phys.* **118**, 10752-10757 (2003).
8. X. Chécoury, S. Enoch, C. López, A. Blanco, "Stacking patterns in self-assembly opal photonic crystals," *Appl. Phys. Lett.* **90**, 161131 (2007).
9. A. Balestreri, L. Andreani, M. Agio, "Optical properties and diffraction effects in opal photonic crystals," *Phys. Rev. E* **74**, 036603 (2006).
10. F. García-Santamaría, J. F. Galisteo-López, P. V. Braun, C. López, "Optical diffraction and high-energy features in three-dimensional photonic crystals," *Phys. Rev. B* **71**, 195112 (2005).
11. A. F. Koenderink, A. Lagendijk, W. L. Vos, "Optical extinction due to intrinsic structural variations of photonic crystals," *Phys. Rev. B* **72**, 153102 (2005).
12. J. F. Galisteo-López, M. Galli, M. Patrini, A. Balestreri, L. C. Andreani, C. López, "Effective refractive index and group velocity determination of three-dimensional photonic crystals by means of white light interferometry," *Phys. Rev. B* **73**, 125103 (2006).
13. L. Dorado, R. A. Depine, H. Míguez, "Effect of extinction on the high-energy optical response of photonic crystals," *Phys. Rev. B* **75**, 241101(R) (2007).
14. K. Ohtaka, "Scattering theory of low-energy photon diffraction," *J. Phys. C: Solid State Phys.* **13**, 667-680 (1980).

15. N. Stefanou, V. Yannopoulos, A. Modinos, "Heterostructures of photonic crystals: frequency bands and transmission coefficients," *Comput. Phys. Commun.* **113**, 49-77 (1998);
16. N. Stefanou, V. Yannopoulos, A. Modinos, "MULTTEM 2: A new version of the program for transmission and band-structure calculations of photonic crystals," *Comput. Phys. Commun.* **132**, 189-196 (2000).
17. L. Dorado, R. A. Depine, H. Míguez, "Resonant multipole effects in monolayers of periodically arrayed dielectric spheres", *Phys. Rev. B* (2007, submitted).
18. M. Inoue, "Enhancement of local field by a two-dimensional array of dielectric spheres placed on a substrate," *Phys. Rev. B* **36**, 2852-2862 (1987).
19. T. Kondo, M. Hangyo, S. Yamaguchi, S. Yano, Y. Segawa, and K. Ohtaka, "Transmission characteristics of a two-dimensional photonic crystal array of dielectric spheres using subterahertz time domain spectroscopy," *Phys. Rev. B* **66**, 033111 (2002).
20. B. Gralak, D. Maystre, "Electromagnetic phenomenological study of photonic band structures," *J. of Modern Optics* **47**, 1253-1272 (2000).

The so-called high energy range of three-dimensional (3D) photonic crystals (PCs), where the lattice constant is on the order of, or greater than, the wavelength of light, presents a myriad of potential technological applications whose exploration has just started. The advent and subsequent improvement of fabrication techniques that take advantage of self-organizing properties of dielectric spheres in the micrometer scale have permitted to obtain high quality colloidal crystals, which have been thoroughly studied in the low energy range [1-4]. However, many reported optical properties in the high energy range remain unsatisfactorily explained and there is a lack of proper theoretical guidance for experimentalists working in the field. In this high energy region, in spite of the absence of gaps or pseudo-gaps in the photonic band structure, the appearance of peaks in the reflectance spectra (dips in the transmittance spectra) have attracted much attention in the last years [5-9]. In that same range, the effect of coherent scattering is also observed for non-forward directions, for which optical diffraction patterns have been reported [10]. Efforts have mainly been focused on finding an explanation of the origin of these optical features by using approaches based on the comparison between the measured spectra and the calculated band structure [4,10]. However, these attempts have not provided a satisfactory description of the physical origin of all these features. Very recently, we found that the comparison between the spectra and the band structure has little sense if intrinsic defects are not taken into account, a realistic physical description of the system requiring the modeling of imperfections or disorder in some way. The density of defects that is present in real crystals can be simulated by adding optical extinction into the theoretical model [11-13]. This changes drastically the higher order band structure with respect to the case of a perfectly ordered crystal [13], a clear correspondence between the maxima of the imaginary part of the wavevector in the complex band structure and the pattern of maxima and minima observed in the optical spectra being established. Nevertheless, this approach does not permit to recognize the fundamental interactions that originate each peak or dip in the spectra. It is the aim of the present work to clearly establish the physical origin of the high energy optical response of 3D sphere PCs.

The approach we will follow here takes advantage of the multipole expansion of the electromagnetic field used in the frame of the vector Korringa-Kohn-Rostoker (KKR) method in its layer version [14-16]. The crystal slab is first divided into layers parallel to a given crystallographic plane, each layer containing an infinite number of periodically arrayed identical spheres. Next, a doubling-layer scheme is used to obtain the reflection and transmission matrices of the multilayer from the matrix elements of a single layer.

In the multipole expansion of the electromagnetic field, each pair of integers (l, m) , where $l \geq 1$ and $-l \leq m \leq l$, represents a spherical partial wave or multipole field of order (l, m) , which can be either electric or magnetic. By summing up the $2l+1$ electric and magnetic partial waves of the same l , the field of a 2^l -pole is obtained, the first four lowest order multipoles being dipoles ($l=1$), quadrupoles ($l=2$), octupoles ($l=3$), and sedecimipoles ($l=4$). Electric multipoles produce always transverse magnetic (TM) fields, while magnetic multipoles produce transverse electric (TE) fields, so this multipole expansion can also be

viewed as a linear combination of TM and TE spherical waves. Therefore, the total scattered field by a sphere is obtained by summing the TM and TE contributions of all 2^l -poles, from $l = 1$ to infinity. In a numerical calculation, a finite cut-off L_{MAX} must be chosen, retaining the first L_{MAX} ($L_{MAX} + 2$) TM and TE terms. Thus, in the vector KKR method, each sphere is approximated by a linear combination of multipoles and the multiple scattering between them within a layer is computed by using their radiated spherical waves. This decomposition into TM and TE modes allows one to address resonance phenomena inside the crystal slab by separating and classifying the multipoles and their respective TM and TE contributions that are involved in the response of the system.

We chose a face centred cubic (fcc) lattice of spheres with dielectric constant $\epsilon_s=2.5$ embedded in air, which would correspond to latex spheres (refractive index $\cong 1.58$) arranged in a colloidal crystal. Typically, the crystalline direction perpendicular to the substrate the lattice is deposited on is the [111]. We will focus on the optical properties when light impinges in that particular direction since several measurements are available in the literature in the range of energies we are interested in. Thus, each crystal layer consists of a triangular lattice of close-packed spheres and the slab width is increased by piling layers up in the known sequence ABCABC... As it is usual, the photon energy is expressed in reduced units a/λ where a is the lattice constant of the classical cubic cell, whose value is $a=2\sqrt{2}S$ in an fcc close-packed structure, S being the sphere radius and λ the wavelength of the incident light.

We make use of previous results extracted from an exhaustive analysis of the optical properties of the monolayer [17]. First, we briefly recall the theoretical analysis of self-standing slabs because the behaviour of slabs deposited on dielectric substrates [17] can be understood from them by applying the same procedure described here and by taking into account the interaction with the substrate. Also, in order to separate the contributions of the lowest order multipoles, which are electric and magnetic dipoles, we have to reduce the sphere size of a close-packed structure while maintaining, however, the positions of the original sphere centres. Under this condition, each sphere in the lattice can be replaced with electric and magnetic dipole moments by setting a cut-off $L_{MAX}=1$ in the multipole expansion.

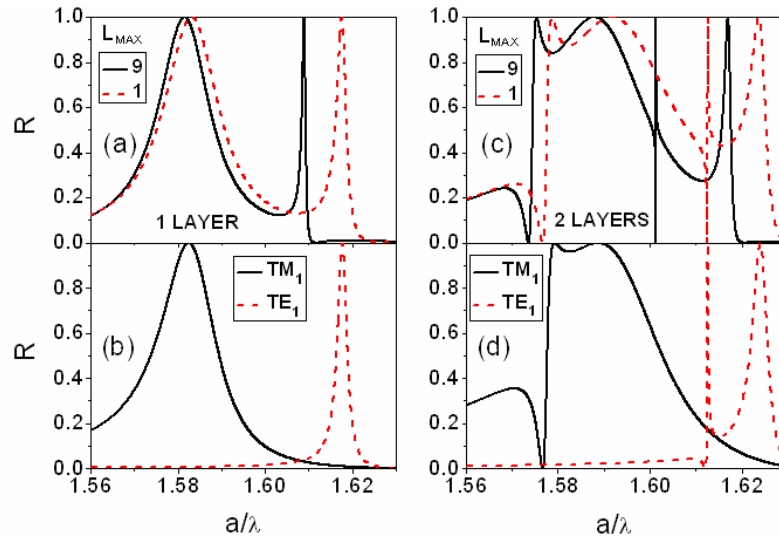


Fig. 1. (a) Comparison between the reflectance spectrum ($L_{MAX}=9$) and its dipolar contribution ($L_{MAX}=1$) of a self-standing monolayer ($N=1$) for energies just below the diffraction cut-off. (b) TM and TE dipolar contributions to the reflectance spectrum in (a). (c) Comparison between the reflectance spectrum ($L_{MAX}=9$) and its dipolar contribution ($L_{MAX}=1$) of a self-standing bilayer ($N=2$) for energies just below the diffraction cut-off. (d) TM and TE dipolar contributions to the reflectance spectrum in (c). The sphere radius and dielectric constant are $S = 0.15a$ and $\epsilon_s = 2.5$, respectively, while the embedding medium is air.

In Fig. 1(a), the calculated specular reflectance spectrum of a self-standing monolayer of small spheres $0.15a$ in radius arrayed in a triangular lattice is shown (black solid line), where the distance between sphere centres is $a/\sqrt{2}$. Very good convergence is obtained by using $L_{MAX}=9$, so this is practically the actual response of the system, which is shown for those energies below the onset of diffraction spots located at $a/\lambda=1.63$ [13]. The spectrum obtained by replacing each sphere with equivalent electric and magnetic dipoles is also shown (red dashed line, $L_{MAX}=1$), where a broad and a sharp peak can be observed in agreement with the case $L_{MAX}=9$. This is an indication that dipolar interaction is the only responsible for the appearance of these two peaks, because none other peaks arise when higher order multipoles are added to the description of the system. Under this condition, we could eliminate all the magnetic dipoles from the spherical wave expansion used in the vector KKR method in order to isolate the contribution of electric dipole moments. When this is done, the remaining electric dipoles, which reradiate only TM fields, produce the broad peak in the reflectance spectrum, as can be seen in Fig. 1(b) (black solid line). On the other hand, if all the electric dipoles are removed from the system, the TE fields of the remaining magnetic dipoles produce the sharp reflectance peak observed in Fig. 1(b) (red dashed line). These electric and magnetic dipolar contributions are denoted TM_1 and TE_1 , respectively. Thus, by comparing Figs. 1(a) and 1(b), we realize that the broad reflectance peak is due to the resonance of TM_1 modes, while the sharp reflectance peak originates from the resonance of TE_1 modes inside the monolayer. Because each small sphere behaves like two uncoupled electric and magnetic dipoles, when an incident plane wave impinges on the monolayer, the induced electric dipoles are forced to oscillate harmonically in the same direction of the incident electric field vector, while the induced magnetic dipoles oscillate in the direction of the magnetic field vector. If the incident plane wave is carrying a purely real power density, its electric field vector will be perpendicular to the magnetic field vector in space, both fields being also in time-phase. Therefore, the induced electric and magnetic dipole moments will also be perpendicular to each other, but their phases will in general be different between them and different with respect to the incident fields. Although the incident electromagnetic field imposes the frequency of these dipolar oscillations, the induced dipoles cannot follow the oscillation of the incident field in time-phase at all frequencies, because each dipole in the lattice, either electric or magnetic, is linked to the others through electromagnetic interactions. There exists, however, a particular frequency at which electric dipoles oscillate in time-phase with the incident electric field, producing maximum reflected field intensity due to constructive interference of the reflected waves. This is a resonance phenomenon characterized by constructive interference of TM fields reradiated by electric dipoles, and then we called it a TM_1 resonance. The same happens for the magnetic dipoles, that is, when they oscillate in time-phase with the incident magnetic field, a TE_1 resonance is obtained. The resonance frequency depends on the refractive index contrast and the geometry of the lattice and, consequently, an equivalent red-shift in frequency could be achieved by either increasing the sphere size or reducing the number of nearest neighbours in the lattice.

The same decomposition into TM and TE dipolar contributions can be done for a bilayer composed of small spheres ($S=0.15a$), as can be seen in the specular reflectance spectrum of Figs. 2(c) and 2(d), where two TM_1 and two TE_1 peaks appear in this case due to the interaction between the two layers. Therefore, we can predict that several resonance peaks in the reflectance spectrum will appear as the slab width is gradually increased by piling monolayers up in order to build a 3D periodicity. Moreover, if now we increase the sphere radius up to the greatest possible value in order to obtain a close-packed structure, higher order multipoles must be added to the description of the system, giving rise to even more resonance peaks related to these higher order multipoles. For the refractive index contrasts we are interested in, we found that sedecimipoles are the highest order multipoles that produce the appearance of new resonance peaks of TM and TE nature inside the crystal slab. These multiple resonances due to both the first four multipoles and the increase in the slab width, can be appreciated in Fig. 2 where the calculated specular reflectance spectra for close-packed slabs of $N=1, 2, 3$, and 21 layers are presented. In the case of the close-packed monolayer in

Fig. 2(a), the first peak located at about $a/\lambda=1.18$ is doubly degenerated and originates from the TM_1 and TE_1 peaks in Fig. 1(a), which now have shifted to a lower frequency as a consequence of the interaction with higher order multipoles. In the work by Inoue [18], the frequency shift of the reflectance peaks due to a change in the sphere radius is also shown, so these results support the conclusion that interactions between dipoles and higher order multipoles give rise to a shift of the resonances of dipolar origin. Therefore, the spectral features obtained for small spheres are also present in the case of a close-packed structure having larger spheres. Besides, the eigenstate of the close-packed structure at resonance is not purely TM nor TE, but a linear combination of them in which only one predominates. For this reason, each reflectance peak can be characterized as either TM or TE in origin, both modes being of dipolar nature for small spheres.

We must point out that the resonances of the system are far from the Mie resonances of a single sphere due to the low dielectric constant we have chosen. Then, our conclusions apply exclusively under this condition. For the case of high dielectric constant, Kurokawa et al. [3] have shown that the single-sphere Mie resonances survive in the arrayed structure by rigorously calculating the internal electromagnetic field distribution. In that case, resonances could be characterized according to the Mie resonant modes of individual spheres.

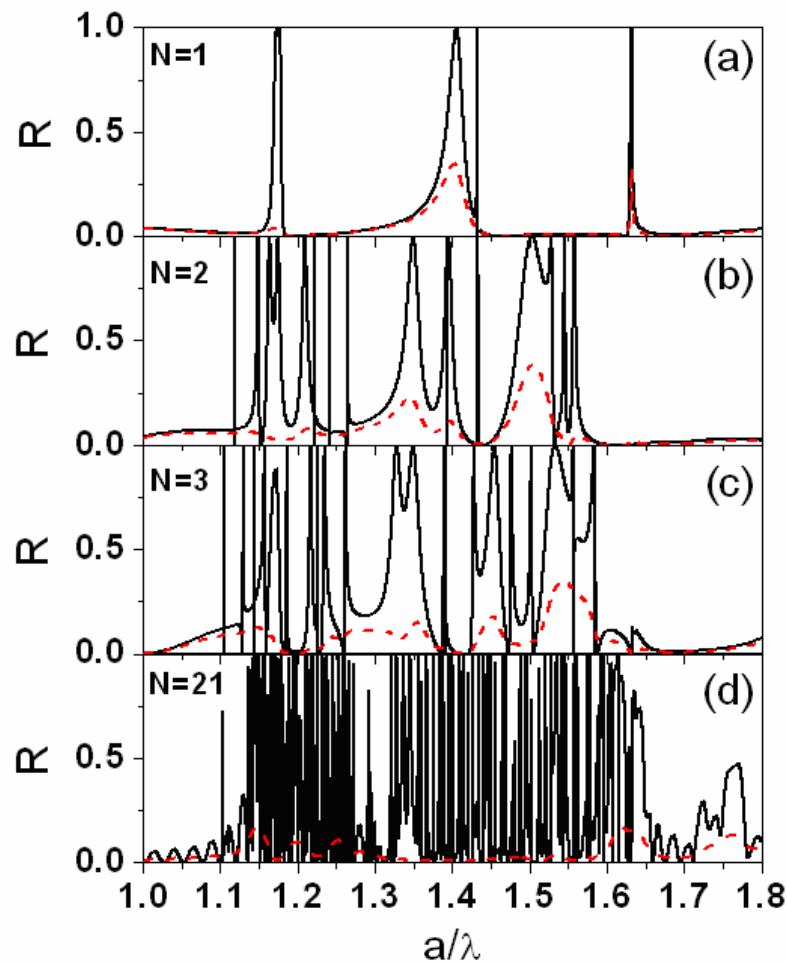


Fig. 2. Specular reflectance spectra for self-standing slabs of close-packed spheres of dielectric constant $\epsilon_s=2.5$ (black solid lines) and $\epsilon_s=2.5+0.04i$ (red dashed lines) in air. (a) $N=1$, (b) $N=2$, (c) $N=3$, (d) $N=21$ layers.

Figure 2 (red dashes lines) also shows the spectra when disorder effects are taken into account by introducing extinction in the theoretical model via an imaginary part $\varepsilon_i=0.04$ added to the dielectric constant of the spheres [19], which is a value that has provided good agreement with experiments [13]. In this case, since absorption in the sphere material is negligible in the spectral range under analysis, the imaginary part of the sphere dielectric constant accounts for the extinction caused by diffusely scattered light produced by disorder and imperfections in the crystalline structure, which removes energy from the specularly reflected and forward transmitted beams. Nevertheless, contributions from different types of imperfections cannot be isolated by means of this single parameter. We can appreciate that disorder has a dramatic effect on the shape of the spectra, smoothing sharp resonances so strongly that they practically disappear. A great attenuation of the reflectance values can also be observed with remaining small peaks that are a resemblance of broad resonances, TM in origin most of them. In the case of the slab 21 layers wide in Fig. 2(d), only three small peaks near $a/\lambda=1.2$ and two peaks above $a/\lambda=1.6$ have survived to the extinction. Thus, the highly fluctuating behaviour of the reflectance spectrum in Fig. 2(d), due to the appearance of multiple resonances, is drastically smoothed by the presence of disorder.

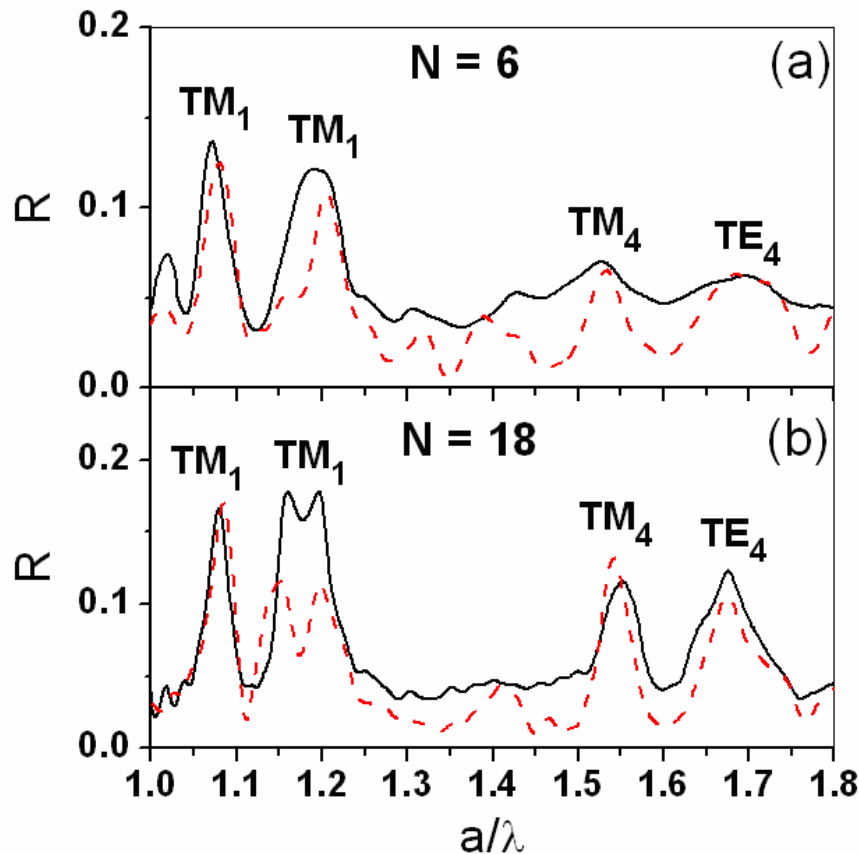


Fig. 3. Measured (black solid lines) and calculated (red dashed lines) specular reflectance spectra for glass-supported slabs of close-packed spheres of dielectric constant $\varepsilon_s=2.5+i\varepsilon_i$ in air. (a) $N=6$ layers, $\varepsilon_i=0.08$, (b) $N=18$ layers, $\varepsilon_i=0.06$.

The same method applied to the determination of the TM and TE dipolar contributions to the resonance peaks in the reflectance spectra in Fig. 1 can be used for higher order multipoles even when the effect of disorder is taken into account and when the slab is deposited on a

dielectric substrate. The measured (black solid line) and calculated (red dashed line) specular reflectance spectra for a slab 6 layers wide deposited on a glass substrate (refractive index = 1.53) are plotted in Fig. 3(a). Details on the PC preparation procedure are provided in detail elsewhere [4]. The good agreement between theory and experiment has been obtained by adding an imaginary part $\varepsilon_i=0.08$ to the dielectric constant of the spheres. The first two peaks located at about $a/\lambda=1.08$ and $a/\lambda=1.2$ are TM_1 in origin, while the very small peaks located between $a/\lambda=1.25$ and 1.5, which are almost imperceptible in the measured spectrum, are mostly TM in origin due to quadrupolar and octupolar interactions, since TE resonances are much more attenuated than TM ones. There is also a small peak at about $a/\lambda=1.54$ that originates from a resonance of sedecimupolar ($L_{MAX}=4$) TM modes (denoted TM_4), that is, electric sedecimupoles are responsible for this peak. Also, magnetic sedecimupoles produce a reflectance peak at $a/\lambda=1.68$, which is then TE in origin (denoted TE_4). The addition of more layers than six does not produce a significant change in the reflectance spectrum, as can be seen in Fig. 3(b) for a slab 18 layers wide ($\varepsilon_i=0.06$), because electromagnetic waves penetrate into the crystal slab down to practically the first six layers when extinction is introduced in the theoretical model and, consequently, the interaction with the supporting glass is practically negligible. The only difference with Fig. 1(a) is that the peak at about $a/\lambda=1.2$ has become doubly degenerated, but it is still TM_1 in origin. We should point out that in Ref. [20] a phenomenological theory of 1D PCs is developed, where resonances associated with poles and zeros in the complex plane of the wavevector are analyzed in order to explain transmission gaps, which are due to the stacking of homogeneous layers. Although the qualitative aspects of the theory could also be applied to 3D PCs, the resonances of sphere-based PCs are of a fundamentally different origin in the high energy range. Besides, the method of recognition of the resonant electromagnetic modes we have described could also be applied to 2D and more general 3D PCs by using an appropriate expansion into TM and TE modes in each case.

In summary, we presented for the first time a rigorous and general explanation of the physical origin of the optical response of sphere PCs in the high energy range, where previous attempts based on just the photonic band structure provided misleading results. The physical mechanisms we described here are based on collective properties of the lattice dynamics, no matter what the geometric details of its individual components are. Therefore, beyond the specific type of PC we addressed, we expect our conclusions can be generalized to any type of 2D or 3D structure. We found that each peak or dip in the spectra originates from the resonance of a specific mode inside the crystal slab, which resonates as a whole entity due to electromagnetic links between the lattice components.

Acknowledgments

This work has been realized in the framework of a joint Spanish-Argentinian cooperation project CSIC-CONICET (Grant 2005AR0070). RAD and LD acknowledge support from Consejo Nacional de Investigaciones Científicas y Técnicas (CONICET), Universidad de Buenos Aires (UBA) and Agencia Nacional de Promoción Científica y Tecnológica (ANPCYT-BID 802/OC-AR03-14099). HM thanks financial support from the Ramón Areces Foundation and the Spanish Ministry of Science and Education under grant MAT2005-03028.